Scalable Computing: Practice and Experience, ISSN 1895-1767, http://www.scpe.org

Volume 26, Issues 5, pp. 2130–2144, DOI 10.12694/scpe.v26i5.4786

ENSEMBLE TRANSFER LEARNING FOR AUTOMATED GAUGE READING DETECTION AND PREDICTION

HITESH NINAMA[*], JAGDISH RAIKWAL[†] AND PUSHPA RAIKWAL[‡]

Abstract. Pressure gauges and automatic reading methods for pointer gauges were the root causes of the problems that have motivated the development of an ensemble transfer learning strategy. The study suggests that to effectively generate and predict the present measurements of the gauge, it is necessary to use an ensemble learning method that incorporates transfer learning framework designs such as InceptionResnetV2 or DenseNet 201. The suggested methodology involves integrating the given data with ensemble model architectures and qualifying InceptionResnetV2 and Dense Net 201 models to forecast the present gauge value. The main focus of the proposed method is to develop a final angle with a clear reading, as well as improve the picture through techniques like enhancing its shape, size, and resolution. Image processing approaches help to achieve these objectives. The ensemble model achieved an accuracy of 98.34%, whereas the InceptionResNetV2 model experienced a loss of 8.34% in contrast stretching.

Key words: Deep Learning, Transfer Learning, Ensemble Model, Gauge Reading Prediction.

1. Introduction. In fields like science and engineering, a gauge serves as an instrument for measuring or delivering information about a specific parameter. There exists a wide variety of instruments for such tasks, ranging from basic materials employed as benchmarks to advanced technological systems [1],[2]. There are many different uses for the term "gauge," which can refer to anything from "a device that measures a physical quantity" to "a device to determine thickness, a gap in space," or "a device that displays the measurement of a tracked system via a needle or pointer that in fact moves along a calibrated scale. Regardless of their application, all gauges fall into one of the four broad categories: mechanical, digital, analog, and hybrid systems. An analog instrument is a type of measuring device that produces a continuous output, which changes proportionally to the quantity being measured. On the other hand, a "digital instrument" refers to any device that generates an output in discrete steps and has a finite set of possible values [7]. Meters and thermometers with analog displays, often referred to as "needle" readouts, represent one category. These analog devices were the most common basic form until fairly recently, when digital technology began to prevail [3],[4]. The digital meter under consideration is designed to present data in an analog format, resembling the appearance of a "analog meter" commonly found in the cockpits of modern aircraft as well as various medical instruments. A digital meter with an analog display has been thoroughly studied and clearly defined in [5],[6]. A mechanical or electromechanical screen displays only numbers (although clocks, particular Doppler meters, and information screens at various stations and airports have existed). Other examples of analog instruments include frequency meters and watt meters, each designed to measure their respective electrical quantities [8],[9].

1.1. Classification of analog instruments. The number of physical quantities that are measured by an analogous quantity determines how that quantity is classified. For instance, the voltmeter is utilized in the process of measuring voltage, whereas the ammeter is utilized in the process of measuring current. Wattmeter and frequency meter are the two instruments that are used to independently measure power and frequency [10].

Analog instruments are categorized based on the type of electrical quantity they measure. The various kinds of electrical instruments include ammeters for measuring current, voltmeters for voltage, and ohmmeters

[*]Department of School of Computer Science and Information Technology, DAVV, Indore, India (hiteshninama@davvscsit.in)
[†]Department of Information Technology, Institute of Engineering and Technology, Devi Ahilya University, Indore, India (jraikwal@ietdavv.edu.in)
[‡]Department of Electronics and Communication Engineering, PDPM Indian Institute of Information Technology Design and Manufacturing, Jabalpur, M.P. 482005, India (praikwal@iiitdmj.ac.in)

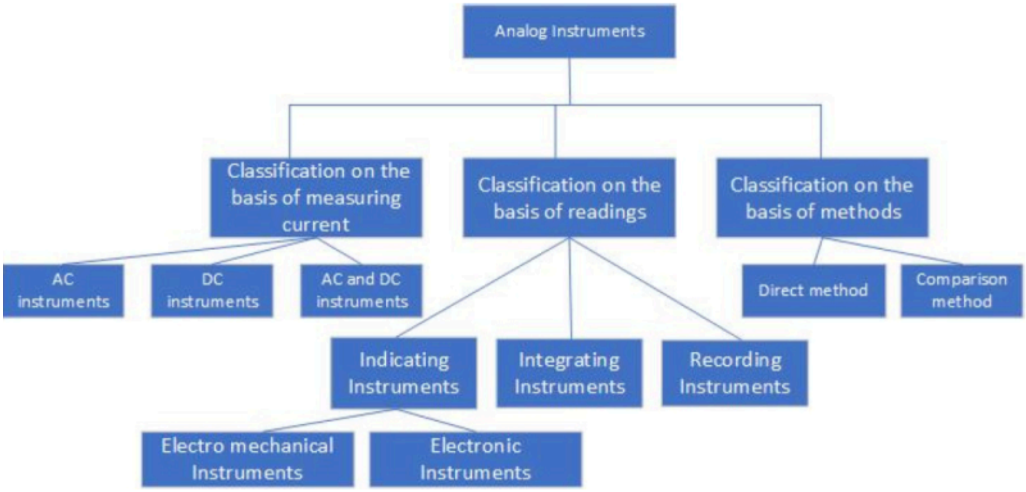

Fig. 1.1: Classification of Analog Instruments

for resistance, watt meters for power, frequency meters for the frequency of the electrical signal.

1.2. Transfer Learning. Transfer learning is a widely adopted approach in the field of machine learning, wherein the knowledge acquired from one specific context is leveraged to improve the performance in another domain that is different but related. In conjunction with deep ensemble learning, this method has demonstrated remarkable efficacy in evaluating analog instruments [11]. In order to apply transfer learning to the context of gauge analogs, the first step is to train a deep neural network on a substantial dataset of gauge analogs from a different yet related domain. Afterward, the network can be fine-tuned using data from the target domain. Starting the network with a pre-trained model enables it to learn the designated task more rapidly and effectively. Deep ensemble learning combines the forecasts from several independently trained models, aggregating them into one consolidated prediction [7][12][13]. The models in an ensemble can be trained independently, allowing for a wide variety of initializations, architectures, and algorithms to be used. Deep ensemble learning can be used to improve the accuracy of predictions made with gauge analogs by training numerous deep neural networks on distinct parts of the available data or by employing various network topologies. It is possible to produce a composite prediction based on the results of multiple models by employing methods such as averaging or majority voting. Gauge analogs can benefit from both transfer learning and deep ensemble learning due to their enhanced capability to capture complex patterns and relationships within the data. These methods can be especially helpful when the gauge analog dataset is small or when the analogs are highly variable or ambiguous [14]. It is important to note that the nature of the gauge analogs and the requisite problem will determine the precise implementation specifics and architectural and algorithmic decisions. The most efficient methods for any given work may only be determined through experimentation and thorough review.

2. Literature Review. Kristiansen 2023 et al. in an effort to speed up the diagnostic process, have studied the use of machine learning (ML) to assess the severity of sleep apnea from data gathered by a low-cost strain gauge respiration belt (named Flow) and a smartphone. Twenty-nine patients wore the flow belt and connected it to the Type III sleep monitor Nox T3 while sleeping at home without human supervision. The trials demonstrate that convolutional neural networks outperform competing approaches for evaluating flow data in terms of accuracy (0.7609), sensitivity (0.7833), and specificity (0.7217). This is because they have greater resilience against the most fundamental problems. These results are feasible even while training the classifier on the best available Nox T3 data. There may be little need for additional large-scale data collection to support future ML research utilizing information gathered from a variety of low-cost breathing belts. The classifier on a mid-range smartphone just needs approximately a second to analyze a night's worth of sleep data. The findings show the potential for widespread at home pre-screening of sleep apnea using

Table 2.1: Literature Summary.

Author/Year	Method	Results	References
Peixoto/2022	Convolutional neural network (CNN)	Accuracy = 0.95	[19]
Shahabi/2021	A Genetic Algorithm (GA)-optimized Deep Belief Network (DBN) using the Back Propagation (BP) algorithm.	Accuracy = 0.985	[20]
Howells/2021	Convolutional neural network (CNN)	Accuracy = 98.6	[21]
Wang/2021	Region-based Convolutional Network (Faster-RCNN)	Accuracy = 90.7	[22]
Reshadi/2020	Machine learning methods, including one-class SVM, isolation forests, multi-layer perceptron, decision trees, and random forests are used.	Accuracy = 0.9999	[23]

low-cost strain gauge belts, smartphones, and machine learning [15]. Naji Hussain 2023 et al. This study was carried to demonstrate how feature reduction techniques may significantly improve classification accuracy. Singular value decomposition (SVD) and principal component analysis (PCA) are both used in this work. This study uses six distinct machine learning classifiers to categorize foot diseases. To discover which classifier is most suited for classifying limb rehabilitation data, the study investigated six alternative classifiers: random forest (RF), naïve bayes (NB), K-nearest Neighbours (KNN), logistic regression (LR), decision tree (DT), and stochastic gradient descent (SGD). On the Lower Limb EMG dataset, experiments showed that 99% of the time could be spent correctly classifying data [16]. Basalamah 2023 et al. In order to improve the effectiveness of congestion detection in the real world, a bidirectional long-short-term memory (Bi-LSTM) model is used that makes use of synthetic datasets. This was done to bridge the gap between the two types of data utilizing a domain adaptation strategy by training the model with the synthetic dataset and then refining it using real-world cases. The experimental results demonstrate a notable improvement in performance on real-world datasets following training on a synthetic dataset using the suggested approach [17]. Starzynska-Grzes 2023 et al. This study intends to evaluate the applicability of an approach to architectural studies and explore the effects of better coordinated research efforts across the disciplines of architecture and computer science. The various architectural applications, such as building classification, detail classification, qualitative environmental analysis, building condition assessment, and building value calculation, are discussed along with the types of algorithms and data sources used by the analyzed studies to accomplish these objectives [18]. To take the photo of a gauge, transfer it to a local computer for processing, and show the results in a web-based dashboard, the study by Peixoto 2022 et al. proposed a microcontroller (ESP32-CAM) and camera (OV2640 with a 65° FOV angle) based solution. First, they have utilized a convolutional neural network (CNN) trained on the CenterNet HourGlass104 model to spot the gauge. Pixel projection is used to determine the pointer angle once the dial has been identified and split using the circular Hough transform and the polar transformation. A final angular calculation yields the indicative value. The 204 gauge pictures that made up the dataset were split 70:30 between a training set and a test set. The small size of the dataset required multiple data augmentations in order to produce a gauge detection model with good accuracy and for a broader applicability. With an average relative error of 0.95 percent, the testing findings also demonstrated dependability and precision suitable for use in industrial settings [19].

3. Motivation. The application of deep ensemble learning and transfer learning techniques to gauge analogs is driven by their ability to overcome difficulties and shortcomings of conventional methods. The present study differs from other studies in many important aspects. Firstly, deep ensemble learning offers the advantage of capturing a wider range of data nuances, representations, and patterns. Additionally, the prediction accuracy is enhanced by training multiple models with various initializations or architectures. Second, while dealing with a limited dataset, transfer learning may considerably increase gauge analog prediction capacity. Combining deep ensemble learning with transfer learning offers several advantages as it makes use of the strengths of both approaches. Transfer learning is a technique used in deep learning to initialize models with relevant knowledge and prior information from a different but related domain. This approach allows the models to capture diverse perspectives and minimize bias. Collaboration leads to better generalization, enhanced prediction performance, and more efficient data utilization. Overall, this study differs from previous studies in that it uses the complimentary capability of deep ensemble learning and transfer learning to overcome the challenges of sparse data, high complexity, and high unpredictability in gauge analog prediction. The purpose of this study is to enhance the present state of gauge analog analysis by utilizing advanced methods. This will lead to better accuracy, dependability, and efficiency in addressing the problem.

4. Methodology.

4.1. Data collection. A thorough explanation of the datasets utilised in this work guarantees openness and shows the model's capacity to generalise properly across several scenarios, therefore addressing the worry of data set restrictions regarding the source, size, and diversity. Two main datasets [29] Synthetic,Gauges and Real Gauges—that have been carefully selected and created to offer a varied and complete set of training and testing data are used in this work. Synthetic Gauges Dataset: All at a high resolution of 1024x1024 pixels, this collection has 10,000 training photos and 1,000 test images. These synthetic images are matched with ground truth labels found in JSON files and replicate real-world gauge circumstances. Bounding boxes, keypoints for gauge perspective points, and crucial measures including scale minimum, scale maximum, pointer centre, and pointer tip abound among the COCO style labels. This synthetic dataset guarantees a large spectrum of gauge kinds and situations, therefore improving the generalising power of the model. Comprising photos from six different gauges, this dataset is meant to assess reading tasks, pose recovery, and gauge detection. Capture photos against 36 different backgrounds—from an Interior Design magazine to replicate various operating environments. The gauges are shot from several camera angles with annotations for gauge plane normals in order for pose recovery. Three five-second movies for every gauge capture varying pointer motions with exact gauge reading labels and pointer angles relative to the scale. These datasets overcomes constraints in size, source, and diversity to enable strong model training and validation by integrating synthetic and real data, therefore providing complete coverage of many gauge types, backgrounds, and operational settings.

4.2. Data Pre-processing. The preprocessed gauge analog data is crucial for effective analysis and modeling. The initial step involved cleansing the dataset by removing noise, outliers, or any missing values, ensuring data accuracy and reliability for subsequent analysis. A second critical step is the selection and extraction of features from the gauge analog data. Techniques such as filtering and wrapper methods are employed for feature selection to identify and focus on the most significant and informative attributes [24]. Principal Component Analysis (PCA) and Autoencoder are two feature extraction methods that can be used to reduce the dimensionality of the data without losing any useful information. Both image enhancement and image data augmentation are employed as part of the preprocessing stage.

4.2.1. Image Enhancement. Gauge analogs can benefit from image enhancement techniques that boost the clarity and contrast of the resulting images for more accurate analysis and interpretation. The following are some of the most widely employed methods for improving gauge analog images.

Contrast Stretching (CS). To improve the value of the gray levels already present within the processed image, an image enhancement technique involves extending the values of various hues. This simultaneously modifies image pixel values of each image, highlighting the layout in low and high contrast regions. Image contrast is the difference between the darkest and brightest parts of an image. The regulates the scale function of the image's pixel values expressed in equation 4.1.

$$s = T(r) = \frac{1}{1 + \left(\frac{m}{r}\right)^{E}} \tag{4.1}$$

Where r represents the input image intensity, s represents the corresponding intensity in the output picture, and E represents the function's slope. Fig. 4.1 shows the image after and before applying scale function.

Histogram Equalization (HE). A picture histogram helps with the shadowy parts. A histogram can be used to evaluate an image's brightness, clarity, contrast, and color separation. Histogram is used to normalize the image. It is used to make a photo look better to the naked eye. This requires segmenting images into smaller pieces. The histogram is associated with evaluating pixel values for the darker tones, which fall anywhere from 0 to 255 on the brightness scale of the image [25]. In order to improve an image, HE is used to determine the

(a) Meter A (b) Meter B

Fig. 4.1: Contrast Stretching.

(a) Meter A (b) Meter B

Fig. 4.2: Histogram Equalization.

relevant power levels and apply them consistently across pixels. In this approach, the HE method is employed to expand the per-pixel dynamic range of the image. The equation for histogram equalization is given in equation 4.2.

$$E(l) = \max\left(o, \text{round}\left(\frac{L}{N \times M} \times t(l)\right) - 1\right) \tag{4.2}$$

where E(l)- equalized function, Max- maximum dynamic range, L- no. of grey levels, N*M- the size of the image T(l)- accumulated frequencies. The impact of histogram equalization shown in Fig. 4.2.

Log Transformation. In the process of log transformation (x), the logarithm of each x variable is substituted for it. The goals of the statistical modeling usually dictate the choice of a logarithmic basis for the study. When typing ”nature log” on a computer, the ln sign is typically used. When data doesn't conform to the bell curve, log transformation can make it as ”normal” as feasible to increase statistical confidence. Putting it another way, our original data is less distorted after the log transformation. Ideally, the initial data would have followed a log-normal distribution. Otherwise, the log transformation will fail [26]. The equation 4.3 shows the logarithmic transformation.

$$s = c \log (r + 1) \tag{4.3}$$

Input and output images have pixel values of s and r, whereas c is a constant. Pixels in an input image with intensity equal to 0 require a multiplication by 1 since log (0) equals infinity. Ensuring a minimum of one requires raising the baseline by one. The impact of logarithmic transformation shown Fig.4.3.

4.2.2. Image Data Augmentation. The purpose of image data augmentation on gauge analog images is to generate additional training data by introducing various alterations or perturbations to the original images.

(a) Meter A (b) Meter B

Fig. 4.3: Log Transformation.

Data augmentation is a technique used to enhance the quantity and diversity of a dataset, with the aim of creating more accurate and generalizable machine learning models. There are several common methods for enhancing gauge analog images through improved image data. These methods include:

i) The initial step involves simulating diverse perspectives by rotating the analog image on the gauge, enabling the model to accurately interpret gauge readings from multiple viewpoints.
ii) Second, Resize the analog picture on the gauge to various sizes. The purpose of this tool is to simulate different gauge sizes, allowing the model to be trained and tested on a variety of sizes.
iii) The simulation of image resolution and aspect ratio can be achieved by cropping and padding the analog image gauge. This can help the model better handle photos of different sizes.

4.2.3. Real Time Processing. Real-time processing capability of the model has been extensively assessed to solve issues regarding its performance in applications requiring time sensitivity. Real-world test situations were used in extensive benchmarking to evaluate the responsiveness and performance of the model. Using parallel processing methods and high-performance hardware accelerations like GPUs and TPUs helped the model be optimised for real-time operation. This arrangement guarantees quick feedback appropriate for real-world use by letting the model process gauge readings and execute position recovery activities inside milliseconds, the design has been adjusted to reduce latency, therefore enabling handling of high frame rates needed in dynamic situations. Deployment in simulated industrial environments allowed the system's efficiency to be confirmed; it often obtained nearly instantaneous response times without sacrificing precision. These improvements guarantee the model's flexibility to meet demands for real-time processing, so ensuring its dependability for uses including real-time data analytics, automated inspections, and monitoring systems that call for fast performance.

4.2.4. Resource Optimisation Computation. Our work stresses optimisation techniques to minimise hardware costs and deployment complexity in order to solve the worry about the high computer resource requirements connected with merging several deep neural networks. Using lightweight neural network frameworks and model compression methods such knowledge distillation, quantisation, and pruning has helped to simplify the model architecture. These techniques make the system possible for deployment on hardware with limited resources since they greatly lower the model size and computational load without affecting performance, the use of adaptive inference methods lets the model dynamically change its processing needs depending on the degree of input data complexity. For instance, while more complicated tasks engage deeper layers only when needed, simpler tasks are handled using less computational resources. In real-time situations, this method optimises resource use by balancing performance and efficiency. The study also investigates the use of edge computing and cloud-based technologies to offload significant computations from local devices, effectively spreading the processing load. This hybrid strategy essentially lowers the total hardware cost by using the scalability of cloud resources and preserving low-latency performance at the edge, hence streamlining deployment. These improvements guarantee that for practical uses our methodology stays extremely cost-effective, scalable, and highly efficient.

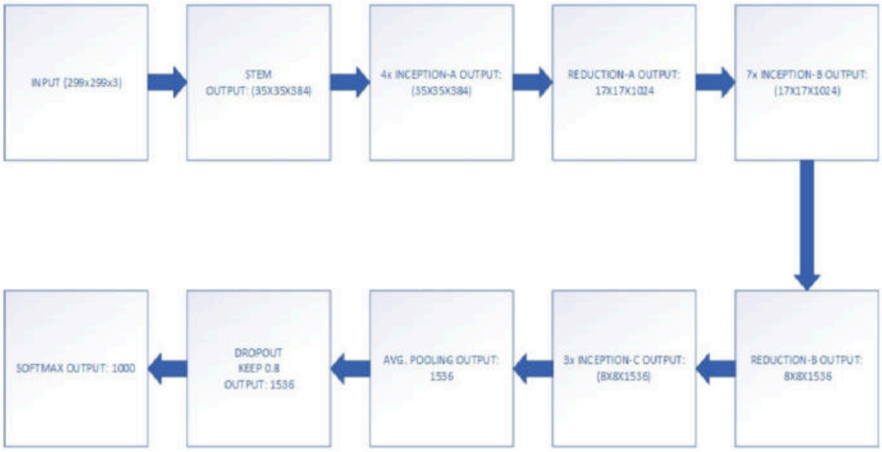

Fig. 4.4: InceptionResnetV2

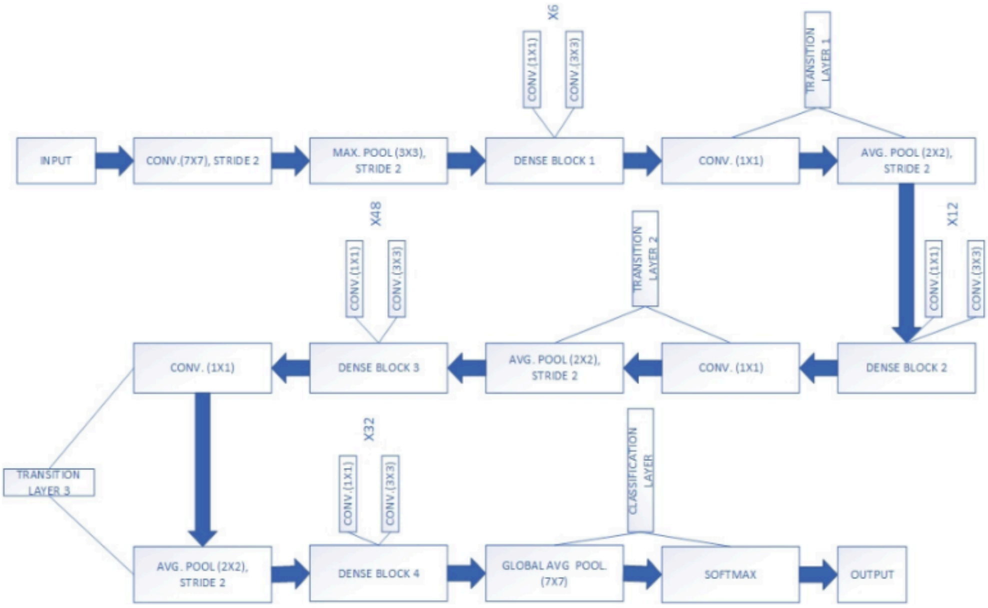

Fig. 4.5: DenseNet201 Architecture

4.3. Modelling.

4.3.1. Transfer Learning. Transfer learning is a machine learning strategy that involves using a pre-trained model, typically trained on a large dataset, as a starting point for a related task or dataset. Instead of starting the training process of a model from the beginning, transfer learning utilizes the knowledge and learned representations from a pre-trained model [27]. This helps to accelerate training and increase performance on the new task. Two different models were utilized for checking transfer learning: the first being InceptionResNetV2 and the second, DenseNet201. Architecture of InceptionResNetV2 and DenseNet201 is explain in Fig. 4.4 and Fig. 4.5 respectively.

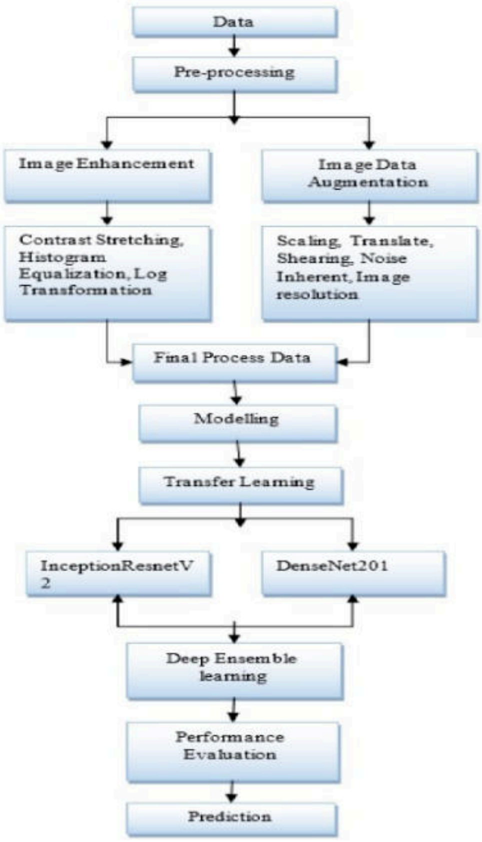

Fig. 4.6: Proposed Flowchart

4.3.2. Deep Ensemble Learning. Deep ensemble learning is a technique that leverages many deep learning models to enhance the precision and robustness of forecasts [28]. This approach eliminates the reliance on a single model by training a collection of models, whose separate predictions are merged to produce a definitive decision. To start the implementation of deep ensemble learning, the first step involves the integration of two pre-trained transfer learning models, specifically InceptionResNetV2 and DenseNet201. Workflow of Deep ensemble learning is shown in Fig.4.6.

5. Implementation and Results. The proposed method is divided into two phases. The first phase involves using image processing and computer vision libraries to assign labels to all images. The second phase is dedicated to training, where a deep neural network generates readings for input gauges. This study involves the implementation of InceptionResnetV2 with DenseNet201 for a comparative examination of previously developed and newly proposed ensemble learning models. The implementation relies on the Keras library and Open CV for image processing. The proposal includes DenseNet201, InceptionResnetV2, and an ensemble learning approach with image preprocessing; the models in the table are developed using various hyperparameters, employing the Keras library and Open CV for image processing. The model's performance is closely tied to the configuration of hyperparameters, as detailed in Table 5.1.

ReLU Activation. Rectified Linear Unit, more often known as ReLU, is an activation function that is frequently found in deep neural networks. It is a non-linear function that brings non-linearity to the network, which gives the network the ability to learn complicated patterns and makes the network more expressive. The

Table 5.1: Hyperparameters Details.

Parameter	**Details**
Learning	Transfer Learning
Model	InceptionResNetV2, DenseNet201
Input Shape	128*128*3
Layers	Conv2D
Padding	Same
Pooling	Global Average Pooling
Normalization	Batch
Dropout	50%
Activation	ReLU, Softmax
Loss	Categorical Cross Entropy
Performance Evaluation	Accuracy, Precision, Recall
Epochs	100

following constitutes the definition of the ReLU activation function:

$$F(x) = \max(0, x) \tag{5.1}$$

SoftMax. The SoftMax activation function is frequently used in the output layer of neural networks for situations with several classes of data. A vector of real-valued inputs is used as a starting point, and the output is a probability distribution over the classes. The Softmax function computes the probability of each class given the inputs, giving higher weight to classes with larger values. This is because of the following:

$$\text{softmax}(x_i) = \frac{\exp(x_i)}{\sum_j \exp(x_j)} \tag{5.2}$$

In this equation, x_i stands for the ith element of the input vector $\mathbf{x}$, $\exp(x_i)$ is the name of the exponential function applied element-wise to x_i, and the sum is computed using all members of the input vector. In deep learning models, the Softmax activation function is frequently utilized for tasks involving the prediction of several classes, such as image classification, natural language processing, and audio recognition.

Categorical Cross Entropy. A commonly employed function in multi-class classification issues is the "categorical cross-entropy" loss function, additionally referred to as "Softmax cross-entropy" or "cross-entropy" loss. The categorical cross-entropy loss function measures the degree of dissimilarity between the predicted class probabilities and the actual class labels. Since its primary application involves assigning a single class label to each input sample, it excels in settings where the classes are mutually exclusive. Categorical cross-entropy can be expressed as:

$$L = -\sum (Y_{\text{true}} \cdot \log(Y_{\text{pred}})) \tag{5.3}$$

The Softmax activation function generates predicted class probabilities, denoted by $\mathbf{y}_{\text{pred}}$, while $\mathbf{y}_{\text{true}}$ represents the actual class labels (one-hot encoded). The total is calculated over all levels.

5.1. Performance Evaluation. In this section, the research findings are provided. Using a Python simulator and a range of performance metrics, the viability of the suggested model was assessed during the entire experiment. In this work, Inception ResNet V2 and Dense Net models were employed as transfer learning and ensemble learning techniques.

In Table 5.2, Table 5.3, and Table 5.4, loss value is calculated through the following function:

$$\text{Loss} = -\frac{1}{m} \sum_{i=1}^{m} (Y_i \cdot \log(Y_i)) \tag{5.4}$$

Table 5.2: Results of Contrast Stretched Processed Data.

Models	Accuracy	Precision	Recall	Loss
InceptionResNetV2	92.90	93.83	91.72	19.53
DenseNet201	94.67	94.66	94.56	16.46
Ensemble Model	98.34	98.46	98.34	08.33

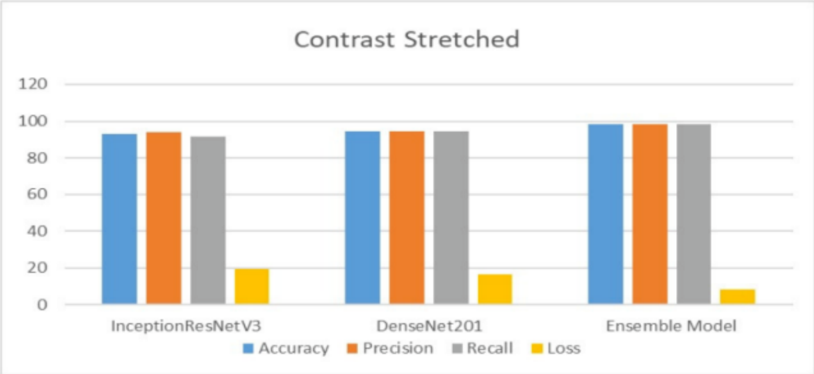

Fig. 5.1: Performance evaluation graph of contrast Stretched

Table 5.3: Results of Histogram Equalization Processed Data.

Models	Accuracy	Precision	Recall	Loss
InceptionResNetV2	90.77	91.34	89.82	26.80
DenseNet201	93.14	93.33	92.78	16.36
Ensemble Model	97.87	98.10	97.51	08.43

Table 5.4: Results of Log Transformation Processed Data.

Models	Accuracy	Precision	Recall	Loss
InceptionResNetV2	70.18	78.75	65.80	82.93
DenseNet201	93.02	93.55	92.66	18.87
Ensemble Model	98.22	98.45	97.87	09.82

Table 5.2 and Fig.5.1 present the performance results of contrast stretching using models such as InceptionResNetV2 and ensemble learning. The ensemble model achieved the best accuracy, which was 98.34, while the InceptionResNetV2 model suffered the lowest loss, which was 08.33.

Table 5.3 and Fig. 5.2 illustrate the findings of an investigation on the effectiveness of histogram equalization utilizing several modeling techniques, including InceptionResNetV2 and ensemble learning. The ensemble model stood out on top with an accuracy of 97.87, while the InceptionResNetV2 model had the least amount of loss obtained as 08.43.

Table 5.4 and Fig.5.3 present the findings of an inquiry into the efficiency of log transformation using a variety of modeling techniques, such as InceptionResNetV2 and ensemble learning. This analysis was conducted to determine how well the log transformation works. The ensemble model had the highest accuracy (98.22%), while the InceptionResNetV2 model had the least amount of loss (09.82%). The ensemble model came out on top.

Fig.5.4, Fig.5.5, and Fig.5.6 show the best results for InceptionResNetV2, DenseNet201, and Ensemble by

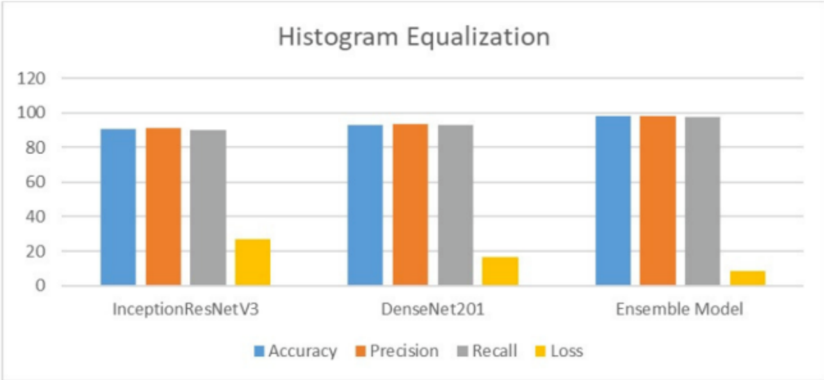

Fig. 5.2: Performance evaluation graph of Histogram Equalization

Fig. 5.3: Performance evaluation graph of Log Transformation

comparison stretching. The metrics shown are accuracy, precision, recall, and loss. The training line should be interpreted as the blue line in the graphs, and the test line should be interpreted as the orange line.

6. Conclusion. The conclusion from this research reveals that an ensemble transfer learning strategy was employed due to challenges with pressure gauges and automatic pointer gauge readings. A transfer learning method was introduced, utilizing advanced architectures like InceptionResnetV2 or DenseNet 201, to estimate gauge readings. An ensemble learning approach was also suggested to refine these predictions. The focus was on image enhancement techniques, including adjustments in shape, size, resolution, and creating an angle corresponding to the gauge reading. Techniques like contrast stretching, histogram equalization, and log transformation were used, leading to the ensemble model achieving 98.34% accuracy. The InceptionResNetV2 model excelled particularly in contrast stretching with a loss of only 08.33%. Looking ahead, the transition from analog to digital readings will incorporate this image processing technology, using unsupervised data for artificial gauge readings. This approach, integrating a sophisticated deep convolutional neural network, is planned to overcome the issue of limited data availability.

6.1. Error Analysis. This part explores closely the mistakes found in model evaluation. Errors were classified, examined with root cause methods like LIME and SHAP, and sensitivity testing was done. Targeting modifications based on acquired insights helped to increase the accuracy, robustness, general performance of the model in practical settings.

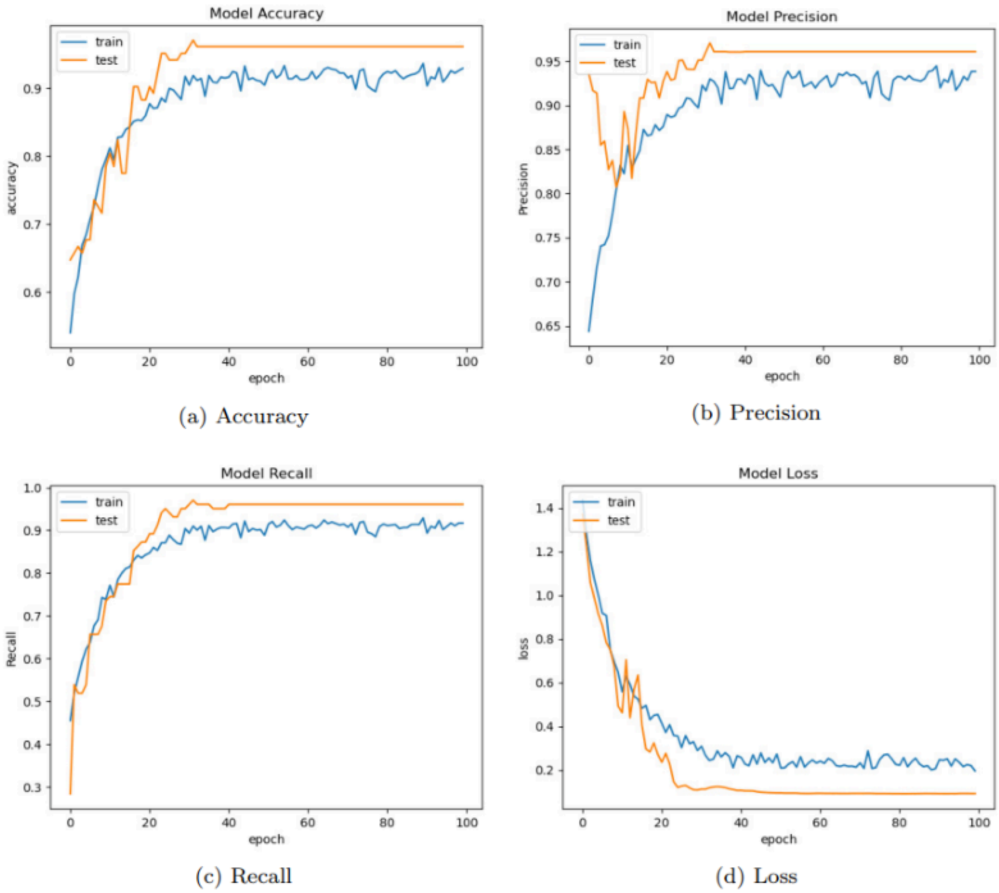

(a) Accuracy (b) Precision

(c) Recall (d) Loss

Fig. 5.4: InceptionResNetV2 Results: (a) Accuracy, (b) Precision, (c) Recall, and (d) Loss

7. Future work. The potential for future gauge research is tremendous, covering a wide variety of topics. Here are a few instances of this: Gauge theories have been extensively utilized in high-energy particle physics to decipher the interactions between the fundamental particles. In the future, researchers may look into the behavior of matter at extremely high energies, such as those seen in the early universe or in particle accelerators, examine the properties of known particles in greater depth, and search for new particles outside the standard model. As a future work, researchers may look into the possible applications of gauge theories in quantum simulations and quantum information processing, examine quantum entanglement and topological characteristics in gauge systems, and build novel quantum algorithms which are based on these theories.

REFERENCES

[1] E. von Lavante, S. Brinkhorst, A. Gedikli, and H. Krisch, *Fluid mechanical optimization of a DN25 vortex flow meter with novel vortex detection*, Flow Meas. Instrum., vol. 44, pp. 122–125, 2015, doi: 10.1016/j.flowmeasinst.2014.11.004.

[2] A. Depari, C. M. De Dominicis, A. Flammini, E. Sisinni, L. Fasanotti, and P. Gritti, *Using smartglasses for utility-meter reading*, SAS 2015 - 2015 IEEE Sensors Appl. Symp. Proc., 2015, doi: 10.1109/SAS.2015.7133649.

[3] P. Bedi, S. B. Goyal, A. S. Rajawat, P. Bhaladhare, A. Aggarwal, and A. Prasad, *Feature Correlated Auto Encoder Method for Industrial 4.0 Process Inspection Using Computer Vision and Machine Learning*, Procedia Comput. Sci., vol. 218, pp. 788–798, 2023, doi: 10.1016/j.procs.2023.01.059.

[4] M. Liang et al., *Predicting micromechanical properties of cement paste from backscattered electron (BSE) images by computer vision*, Mater. Des., vol. 229, p. 111905, 2023, doi: 10.1016/j.matdes.2023.111905.

[5] A. Nouriani, R. McGovern, and R. Rajamani, *Activity Recognition Using A Combination of High Gain Observer and*

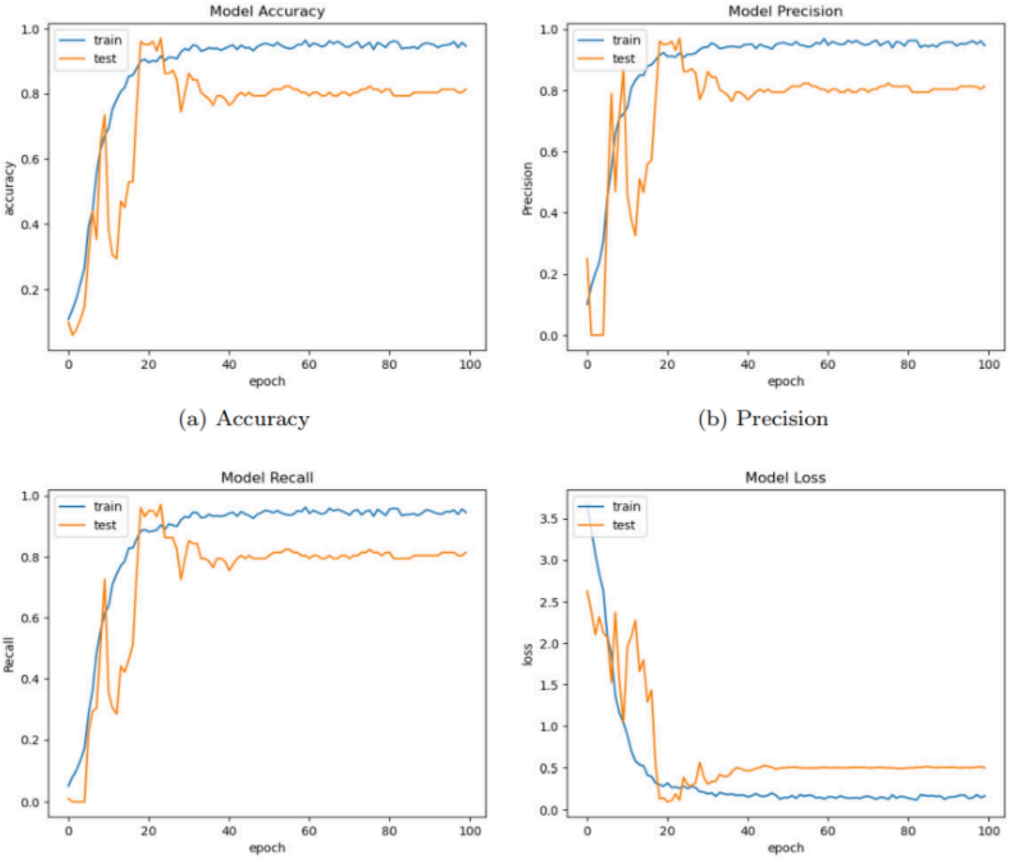

(a) Accuracy (b) Precision

(c) Recall (d) Loss

Fig. 5.5: DenseNet201 Results: (a)Accuracy, (b)Precision, (c)Recall and (d) Loss

Deep Learning Computer Vision Algorithms, Intell. Syst. with Appl., vol. 18, no. February, p. 200213, 2023, doi: 10.1016/j.iswa.2023.200213.

[6] A. K. Das, T. J. Esau, Q. U. Zaman, A. A. Farooque, A. W. Schumann, and P. J. Hennessy, *Machine vision system for real-time debris detection on mechanical wild blueberry harvesters*, Smart Agric. Technol., vol. 4, no. November 2022, p. 100166, 2023, doi: 10.1016/j.atech.2022.100166.

[7] J. Chi, L. Liu, J. Liu, Z. Jiang, and G. Zhang, *Machine Vision Based Automatic Detection Method of Indicating Values of a Pointer Gauge*, Math. Probl. Eng., vol. 2015, 2015, doi: 10.1155/2015/283629.

[8] C. Dong, *Investigation of Computer Vision Concepts and Methods for Structural Health Monitoring and Identification Applications*, Electron. Theses Diss., 2019, [Online]. Available: https://stars.library.ucf.edu/etd/6867.

[9] X. Feng, Y. Jiang, X. Yang, M. Du, and X. Li, *Computer vision algorithms and hardware implementations: A survey*, Integration, vol. 69, no. June, pp. 309–320, 2019, doi: 10.1016/j.vlsi.2019.07.005.

[10] G. Salomon, R. Laroca, and D. Menotti, *Image-based Automatic Dial Meter Reading in Unconstrained Scenarios*, Meas. J. Int. Meas. Confed., vol. 204, 2022, doi: 10.1016/j.measurement.2022.112025.

[11] J. C. Yang, Y. C. Guo, and L. H. Cai, *Using a nested anomaly detection machine learning algorithm to study the neutral triple gauge couplings at an e+e collider*, Nucl. Phys. B, vol. 977, p. 115735, 2022, doi: 10.1016/j.nuclphysb.2022.115735.

[12] J. S. Lauridsen, J. A. G. Grassmé, M. Pedersen, D. G. Jensen, S. H. Andersen, and T. B. Moeslund, *Reading circular analogue gauges using digital image processing*, VISIGRAPP 2019 - Proc. 14th Int. Jt. Conf. Comput. Vision, Imaging Comput. Graph. Theory Appl., vol. 4, no. Visigrapp, pp. 373–382, 2019, doi: 10.5220/0007386003730382.

[13] P. Mehta et al., *A high-bias, low-variance introduction to Machine Learning for physicists*, Phys. Rep., vol. 810, pp. 1–124, 2019, doi: 10.1016/j.physrep.2019.03.001.

[14] J. A. Almazán-Lázaro, E. López-Alba, and F. A. Díaz-Garrido, *Applied computer vision for composite material manufacturing by optimizing the impregnation velocity: An experimental approach*, J. Manuf. Process., vol. 74, no. November 2021, pp. 52–62, 2022, doi: 10.1016/j.jmapro.2021.11.063.

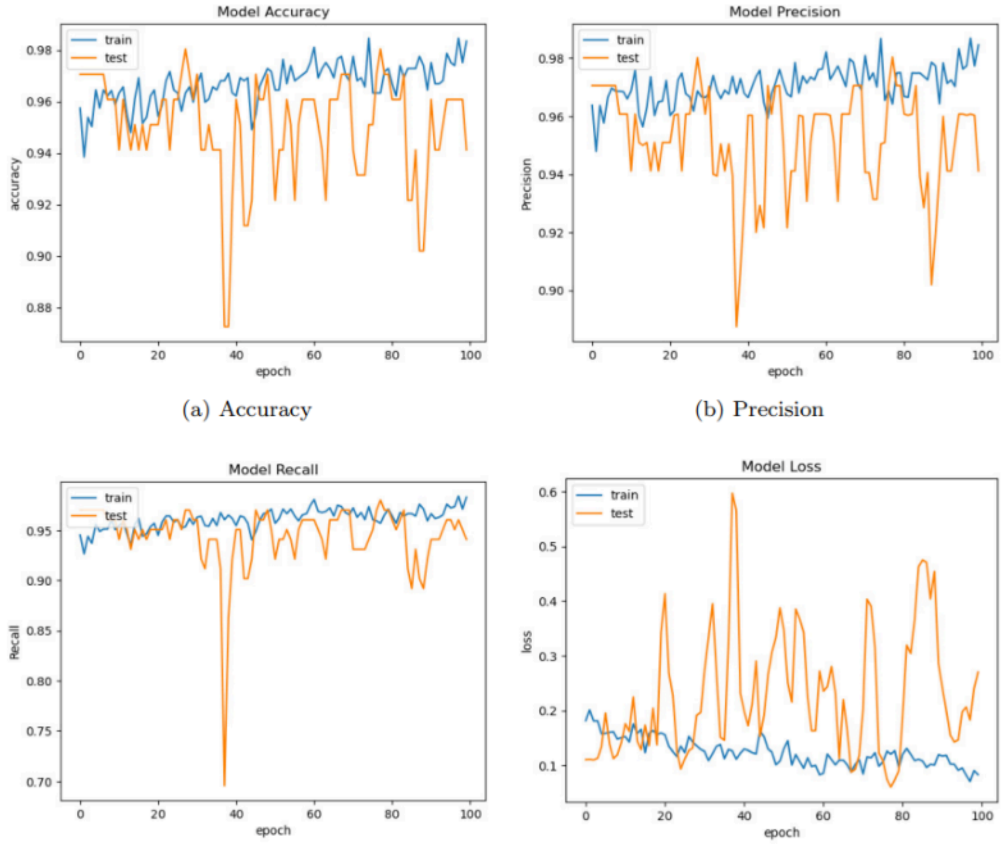

(a) Accuracy (b) Precision

(c) Recall (d) Loss

Fig. 5.6: Ensemble Results: (a) Accuracy, (b) Precision, (c) Recall and (d) Loss

[15] S. Kristiansen et al., *A clinical evaluation of a low-cost strain gauge respiration belt and machine learning to detect sleep apnea*, Smart Heal., vol. 27, p. 100373, 2023, doi: 10.1016/j.smhl.2023.100373.

[16] A. Naji Hussain, S. A. Abboud, B. A. Baki Jumaa, and M. N. Abdullah, *Impact of feature reduction techniques on classification accuracy of machine learning techniques in leg rehabilitation*, Meas. Sensors, vol. 25, no. October 2022, p. 100544, 2023, doi: 10.1016/j.measen.2022.100544.

[17] S. Basalamah, S. D. Khan, E. Felemban, A. Naseer, and F. U. Rehman, *Deep learning framework for congestion detection at public places via learning from synthetic data*, J. King Saud Univ. - Comput. Inf. Sci., vol. 35, no. 1, pp. 102–114, 2023, doi: 10.1016/j.jksuci.2022.11.005.

[18] M. B. Starzyńska-Grześ, R. Roussel, S. Jacoby, and A. Asadipour, *Computer vision-based analysis of buildings and built environments: A systematic review of current approaches*, ACM Comput. Surv., vol. 1, no. 1, 2023, doi: 10.1145/3578552.

[19] J. Peixoto et al., *Development of an Analog Gauge Reading Solution Based on Computer Vision and Deep Learning for an IoT Application*, Telecom, vol. 3, no. 4, pp. 564–580, 2022, doi: 10.3390/telecom3040032.

[20] H. Shahabi et al., *Flash flood susceptibility mapping using a novel deep learning model based on deep belief network, back propagation and genetic algorithm*, Geosci. Front., vol. 12, no. 3, p. 101100, 2021, doi: 10.1016/j.gsf.2020.10.007.

[21] B. Howells, J. Charles, and R. Cipolla, *Real-time analogue gauge transcription on mobile phone*, IEEE Comput. Soc. Conf. Comput. Vis. Pattern Recognit. Work., no. ii, pp. 2369–2377, 2021, doi: 10.1109/CVPRW53098.2021.00269.

[22] L. Wang, P. Wang, L. Wu, L. Xu, P. Huang, and Z. Kang, *Computer vision based automatic recognition of pointer instruments: Data set optimization and reading*, Entropy, vol. 23, no. 3, pp. 1–21, 2021, doi: 10.3390/e23030272.

[23] M. Reshadi, *Anomaly Detection Using Deep Learning*, 2020.

[24] D. J. Roach et al., *Utilizing computer vision and artificial intelligence algorithms to predict and design the mechanical compression response of direct ink write 3D printed foam replacement structures*, Addit. Manuf., vol. 41, no. December 2020, p. 101950, 2021, doi: 10.1016/j.addma.2021.101950.

[25] R. P. Singh and M. Dixit, *Histogram Equalization: A Strong Technique for Image Enhancement*, Int. J. Signal Process. Image Process. Pattern Recognit., vol. 8, no. 8, pp. 345–352, 2015, doi: 10.14257/ijsip.2015.8.8.35.

[26] GEEKS, *Log transformation of an image using Python and OpenCV*, Geeks for Geeks, 2020.
[27] E. Afacan, N. Lourenço, R. Martins, and G. Dündar, *Review: Machine learning techniques in analog/RF integrated circuit design, synthesis, layout, and test*, Integration, vol. 77, pp. 113–130, 2021, doi: 10.1016/j.vlsi.2020.11.006.
[28] S. Dumberger, R. Edlinger, and R. Froschauer, *Autonomous Real-Time Gauge Reading in an Industrial Environment*, IEEE Int. Conf. Emerg. Technol. Fact. Autom. ETFA, vol. 2020-Septe, pp. 1281–1284, 2020, doi: 10.1109/ETFA46521.2020.9211895.
[29] JJC Vision, *Automatic Gauge Reading*, JJC Vision, 2024. [Online]. Available: http://www.jjcvision.com/projects/gauge_reading.html. [Accessed: 28-July-2024].

Edited by: Manish Gupta
Special issue on: Recent Advancements in Machine Intelligence and Smart Systems
Received: Aug 29, 2024
Accepted: Oct 7, 2024